View metadata, citation and similar papers at core.ac.uk

brought to you by CORE

provided by DigitalCommons@WPI

Worcester Polytechnic Institute

Digital WPI

Major Qualifying Projects (All Years) Major Qualifying Projects

2020-05-13

Binder Burnout Investigation on Lanthanum Strontium Manganite

Dominique Meeli Chen
Worcester Polytechnic Institute

Jordan Amir Counsel
Worcester Polytechnic Institute

Kailey R. Catyb
Worcester Polytechnic Institute

Tauny Mackenzie Tambolleo
Worcester Polytechnic Institute

Follow this and additional works at: https://digitalcommons.wpi.edu/mqp-all

Repository Citation

Chen, D. M., Counsel, J. A., Catyb, K. R., & Tambolleo, T. M. (2020). *Binder Burnout Investigation on Lanthanum Strontium Manganite*. Retrieved from https://digitalcommons.wpi.edu/mqp-all/7415

This Unrestricted is brought to you for free and open access by the Major Qualifying Projects at Digital WPI. It has been accepted for inclusion in Major Qualifying Projects (All Years) by an authorized administrator of Digital WPI. For more information, please contact digitalwpi@wpi.edu.

Binder Burnout Investigation on Lanthanum Strontium Manganite

WPI

Binder Burnout Investigation on Lanthanum Strontium Manganite

A Major Qualifying Project

submitted to the faculty of

WORCESTER POLYTECHNIC INSTITUTE

in partial fulfillment of the requirements for the

Degree of Bachelor of Science in Mechanical Engineering

WRITTEN BY:

Kailey Catyb

Dominique Chen

Jordan Counsel

Tauny Tambolleo

ADVISED BY:

Dr. Yu Zhong

Mechanical Engineering Department – Associate Professor

Worcester Polytechnic Institute

May 13th, 2020

This report represents the work of one or more WPI undergraduate students submitted to the faculty as evidence of completion of a degree requirement. WPI routinely publishes these reports on its web site without editorial or peer review. For more information about the projects program at WPI, please see http://www.wpi.edu/academics/ugradstudies/project-learning.html

ABSTRACT

The challenge of efficiently and successfully removing polymer binders within ceramic materials without causing defects or cracks has afflicted its production for decades. It is observed that the heat release and weight loss during the binder burnout (BBO) process are the two dominant parameters that need to be controlled to avoid cracks or fire hazards. The current work investigates the effects of different atmospheric conditions and heating sequences on the heat release and weight loss of Lanthanum Strontium Manganite (LSM), a ceramic oxide that is widely used as the cathode material in solid oxide fuel cells (SOFC). With the use of combination TGA/DSC, a series of experiments were designed to determine how to best control these two parameters, including a benchmark test with dry air and additional experiments using argon, nitrogen, and mixed gas. Furthermore, select experiments were designed with novel customized heating sequences, which may reduce the BBO process time and cost substantially. The results indicated that the heat release and weight loss during the BBO process could be best controlled with either argon or nitrogen as the atmospheric conditions and using customized heating sequences.

AUTHORSHIP

Section	***Author(s)***
Abstract	Tauny and Kailey
Introduction	Tauny
Background	Tauny and Jordan
Methodology	Dominique
Results	Dominique, Kailey, and Jordan
Discussion	All members
Conclusion & Recommendations	Kailey and Tauny

ACKNOWLEDGEMENTS

The authors of this project would like to extend their sincerest thanks to our advisor, Professor Yu Zhong of the Mechanical Engineering Department, for his guidance and continued support throughout the project. We would also like to thank Saint-Gobain Northboro, MA - particularly Mr. Brian Feldman and Dr. John Pietras, for consulting with us throughout our research, providing the sample material, and welcoming us with the utmost hospitality when visiting their labs. Lastly, Mr. Rui Wang, a Ph.D. student in the Integrated Materials and Processes Design (IMPD) Group, deserves special recognition for his mentorship and assistance throughout the entirety of the project, as his contributions were instrumental in our success.

TABLE OF CONTENTS

List of Figures

LIST OF TABLES

1 - INTRODUCTION

As the demand for unconventional materials persists, the desire to manufacture products as efficiently as possible has become a challenge for numerous industries. The manufacturing of ceramic materials, in particular, requires an extensive number of operations that must be carefully controlled to successfully produce the finished product (Reed, 1995). In general, the manufacturing process of ceramic products involves the mixing of raw materials with a binder which is then cast, pressed, or extruded into shape before firing (Alford et al., 1986).

With advanced engineering ceramics, the issue of producing reliable and consistent properties within the product typically results in rejection rates as high as 95%, as even small defects and cracks are sufficient enough to cause failure in a ceramic (Mezquita et al., 2012). Therefore, research into how to prevent defects and cracks has recently become a focus of the ceramic industry.

Most ceramic components are manufactured by using a mechanical or isostatic pressing to shape the powder/binder system (Donzel et al., 2018). For a ceramic green body to have sufficient strength, a binder is added to the dry powder (Ewsuk et al., 1995). However, prior to the sintering stage, any binder must be removed from the green body (Ewsuk et al., 1995). The need to remove the binder is an essential part of ceramic processing, as its presence during the sintering step can result in the final product having defects (Incledon, 2013).

Currently, the most common method for binder removal from a ceramic green body is thermal decomposition. During thermal decomposition numerous reactions occur, releasing gaseous by-products and increasing the pressure within the part (Ewsuk et al., 1995). When the pressure build-up becomes too significant, the part can suffer defects and cracks, thus forcing manufacturers to employ long heating sequences, ranging from 10 to 60 hours, to avoid such issues (Santos et al., 2004). Additionally, the debinding time is greatly influenced by the debinding atmosphere and the type of binder used, as different conditions may produce different reactions (Gonzalez-Gutierrez et al., 2012). Consequently, manufacturers are dependent on previous experience and weight loss data to approximate the heating sequence, which is inefficient and cost-prohibitive. Henceforth, there is a great need to investigate the optimization of binder removal heating sequences.

The goal of this project is to investigate the optimal atmospheric and heating conditions for efficient and effective binder removal. Based on the experimental results and analysis of the collected data, valuable information regarding binder removal can influence the manufacturing and profitability of ceramic products, specifically solid oxide fuel cells (SOFCs). Ultimately, bringing attention to the methods that should be abandoned or adopted to reduce the production time and occurrence of defects.

2 - BACKGROUND

2.1 Advanced Engineering Ceramics

The industry of ceramics dates back to prehistoric times when humans discovered that clay could be mixed with water, formed into objects, and fired. Up until about 50 years ago, ‘ceramics’ were known as porcelain, refractory bricks, cement, and abrasives, but that is no longer the case. More recently, the definition of ceramics has expanded, resulting in the introduction of technical and advanced ceramics.

Due to ceramics' unique properties, such as low thermal and electrical conductivity, high chemical resistance, and high melting point, the use of technical and advanced ceramics has contributed to the growth of many technologically advanced fields. The term ‘advanced ceramics’ dates back to the 1970s and describes crystalline materials with controlled composition and designed with precise attributes (Mason, 2016). In 1975, Ronald Garvie developed phase transformation toughening for partially stabilized zirconia (PSZ), which was a major achievement in the ceramics industry. This allowed for ceramic materials to be created with strength and toughness properties comparable to metals (Wolff, 2018). This achievement, along with many others, allowed for the use of advanced ceramics to expand into a variety of applications and industries. Thus, advanced ceramics are now reliable materials for applications in aerospace, biotechnology, energy, and many other industries.

2.2 Ceramic Powder Shaping

Following the synthesis of the ceramic powder to the desired purity and particle size, the powder can then be shaped using a variety of techniques for processing to form useful final products. In general, the shaping method commonly used for ceramic powders is referred to as powder compaction. Powder compaction (die or isostatic) has become a favorable technique for producing the desired product because it is inexpensive, rapid, and allows for intermediate shape-forming (Niesz, 1996). For proper shaping, the ceramic powder is mixed with processing additives (binders, plasticizers, lubricants, etc.), as the addition of such additives is often required to enhance the ceramic powder forming capabilities (Maleksaeedi & Moritz, 2018). Organic binders, in particular, are used extensively for ceramic shaping processes, creating what is commonly referred to as a ‘binder system’ (Pollinger & Messing, 1985).

2.3 Binders

Binder systems can provide a variety of useful functions in ceramic processing, such as a wetting agent, thickener, suspension aid, liquid retention agent, and consistency aid (Incledon, 2013). However, the main purpose of binders is to provide the green body with sufficient strength to maintain its shape until sintering (Shanefield, 1995). There are several types of organic binders, such as plasticizers, dispersants, wetting agents, etc., but the most commonly used binders are polymers, which are materials composed of very large molecular structures (Lewis, 2001; Incledon, 2013). Some common polymer binders used in ceramics include polyvinyl alcohol (PVA) and polyethylene glycol (PEG) (Lewis, 2001). Typically, binder systems consist of approximately 5 vol.% to 40 vol.% binder, depending upon the formulation method (Lewis, 2001). With the appropriate binder system, the ceramic particles will hold together throughout the shaping stage, after which the binder is removed and prepared for sintering. However, choosing the correct binder can be difficult and many characteristics must be considered, such as green body strength, solubility in fluidizing liquid, and cost (Shanefield, 1995).

The most important characteristic to consider when choosing a binder is its ease of removability (Shanefield, 1995). Following the shaping stage, the polymer binder is removed from the body through a method commonly referred to as thermal debinding or binder burnout (Enneti et al., 2012). Prior to sintering, it is preferred that the binder vaporizes or combusts completely, as to not leave any traces in the fired ceramic, as remnants can result in defects within the final ceramic product (Moeggenborg & Reed, 2002).

2.4 Issues with Current Methods of Binder Burnout

The method of thermal debinding has become a standard among the industry due to its simplicity and applicability for mass production (Enneti et al., 2012). However, thermal debinding does have a variety of drawbacks, as the process itself is very complex and involves both chemical and physical mechanisms (Enneti et al., 2012). One of the main issues with different binder burnout processes is the processing time. To ensure that the binder is removed without causing defects or a build-up of pressure within the body, it is important that the body is heated slowly. With slow heating rates, the risk of a defect or significant pressure build-up occurring is reduced. Although the heating sequences for binder removal have to be slow enough to stay below the critical pressure threshold, they also have to be fast enough to justify the use of binders (Incledon, 2013).

Since there is a variety of ceramics and binders that can be used, their reactions to different heating sequences and different temperatures are unknown. By placing the ceramic green body into a furnace and adjusting the three key variables, temperature, heating rate, and atmospheric conditions, the process of binder burnout is induced. As a result of the decomposition and combustion of the organic compounds in the binder, both heat and mass are released from the green body, which can be tracked using thermogravimetric analysis (TGA) and differential calorimetry analysis (DSC) (Ewsuk et al., 1995). Subsequently, allowing for a better understanding of the reactions occurring and predict the green body's internal behavior when exposed to certain conditions, as this is important for identifying the most effective and safe heating sequence.

2.5 Physics of Thermal Debinding

Thermal debinding occurs throughout three stages at varying temperatures: (1) heat treatment to soften the green body (150 - 200°C), (2) evaporation of the molten binder (200 – 400°C), and (3) evaporation and decomposition of the remaining binder (above 400°C) (Dash, 2011). During the first stage, there is a high risk of encountering reactions that can negatively affect the structure of the body such as shrinkage, deformation, and bubble formation. These reactions are a result of drastic changes in the particle packing and air trapped within the body during the shaping stage (Dash, 2011). During the second stage, capillary flow begins as the binder is extracted from pores to eventually be evaporated. With increasing temperature, the viscosity and surface tension of the molten binder changes, causing the binder vaporization rate to increase. As the binder decomposes and turns into low molecular weight species, it is able to be removed via diffusion or permeation. In the final stage, the residual binder and carbon are removed at temperatures exceeding 600°C (Dash, 2011).

Within the debinding process, there are two limiting factors dependent on sample size, that impact the ease of removal, i.e. transportation and reaction rate. There are two types of thermal degradation that are associated with the transportation of the binder out of the system, i.e. planar-front removal and homogenous removal. Planar-front removal, as shown in Figure 1, assumes that binder decomposition occurs at the outer edges of the body and recedes as a planar-front into the body (Incledon, 2013). Planar-front removal occurs with high thermal resistance when $L^2/ \geq 10^4$ where L is half the body thickness and α is thermal diffusivity (Incledon, 2013). Homogenous removal, however, assumes that there is uniform degradation of the binder throughout the body,

as shown in Figure 2. Since there is no temperature gradient in homogenous removal, the binder reaches its volatilization temperature uniformly.

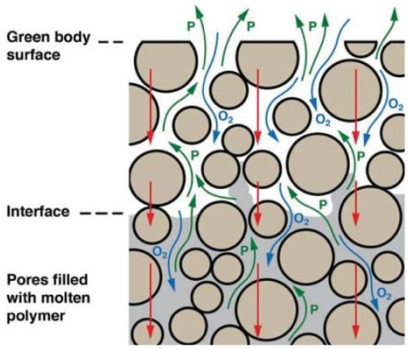

FIGURE 1 – SCHEMATIC EXAMPLE OF PLANAR-FRONT BINDER REMOVAL (SALEHI ET AL., 2012)

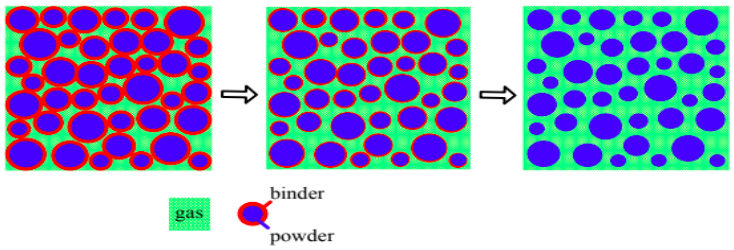

FIGURE 2 – SCHEMATIC EXAMPLE OF HOMOGENOUS BINDER REMOVAL (INCLEDON, 2013)

2.6 Thermal Degradation of Polymers

The behavior of a polymer binder undergoing thermal decomposition is largely dependent on its crystallinity. In this case, the binder is made of acrylic which has an amorphous crystalline structure. Acrylic undergoes a second-order transition at 50°C causing it to soften and become rubbery, and further transition to a fluid state at its melting temperature of 100°C (Beyler, 2002). As the temperature continues to rise the binder will undergo several chemical reactions that allow it to be released from the green body.

During thermal degradation, chain scission, the process in which molecules bonded to the long-chain backbone of the polymer begins to break, occurs as a result of high temperatures (Beyler, 2002). Once the polymer reaches the reaction temperature it will degrade either in series or in parallel. In series degradation, the first reaction occurs, creating an intermediate solid and associated volatile species. The intermediate solid has a unique reaction temperature, that when reached creates a second intermediate solid and associated volatile species. In parallel degradation, the first polymer species begins volatilizing and transporting out of the body, while the second species may begin reacting but remains independent of the first species. The multi-step process of parallel degradation can be beneficial because it allows the gas time to diffuse out of the body (Incledon, 2013).

3 - METHODOLOGY

With the recent desire for more sustainable and efficient energy sources, there has been an increased interest in the synthesis and use of SOFCs. One material in particular that has received attention by some manufacturers is Lanthanum Strontium Manganite (LSM). Due to its phenomenal electrochemical and catalytic activity, LSM has shown promise as a cathode material for SOFCs (Zhang, 2019). For this project, samples of LSM were obtained from Saint-Gobain North America to be investigated under simultaneous differential scanning calorimetry (DSC) and thermogravimetric analysis (TGA). This method of thermal analysis measures enthalpy changes due to the temperature evolution of a sample, while TGA is used to measure the changes in the sample's mass. Both parameters can be analyzed simultaneously and evaluated as a function of temperature or time. The output data can then be graphed and used to predict the chemical and physical behavior of the binder material as temperature and atmospheric conditions change, by identifying regions of intense change in enthalpy and mass. However, this method is limiting, because it can only be used on small samples weighing approximately 20 mg. As such, the data is also limiting, preventing it from being scaled up to accurately predict any physical changes or defects in industry sized samples.

FIGURE 3 – TA INSTRUMENTS SDT 650

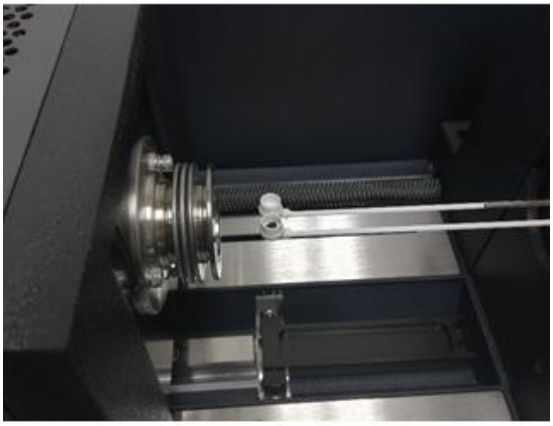

FIGURE 4 – LSM SAMPLE IN AN ALUMINA CRUCIBLE

TA Instruments SDT 650 simultaneous thermal analyzer, as seen in Figure 3, in conjunction with TA Instruments TRIOS software were used to conduct the thermal analysis. In preparation for the experiment, two alumina crucibles were placed on the weighing beams and the instrument was

tared. Using a scalpel and tweezers, a small sample was cut from the corner of the larger LSM sheet and weighed on a digital scale. The LSM sample was cut until the scale read approximately 20 mg. Once the sample measured the appropriate weight, it was placed in the outermost alumina crucible as shown in Figure 4.

The instrument is divided into two chambers, i.e., the sample and balance chambers. In each chamber, gas flows continuously to protect the instrument from rising temperatures. To maintain the mass calibration of the instrument, the gas flow must be equal for each. Using the TRIOS software, the sample flow was set to 100 mL/min to match the Balance Flow. Meanwhile, the Blending Gas Delivery Module (GDM), an external accessory with additional gas ports delivers the gas of choice to the reactive gas port in the TGA. The TGA gas port is compatible with several atmospheric gases such as nitrogen, oxygen, argon, and air, in addition to being capable of blending and delivering gas mixtures with a software-controlled ratio.

Table 1 outlines each experiment conducted, including the ramping rates and chamber gas(es). This design is limited by sample size, as the experiments do not reflect the size of the full LSM sample. As a result, the nature of the thermal decomposition may be affected and possibly not reflect the physical changes that would be observed with a larger sample. However, this data will still reflect the chemical changes of the species and allow for the design of an optimal heating sequence based on the reactivity of the specimen.

TABLE 1 – DETAILED OUTLINE OF THE TGA/DSC EXPERIMENTS CONDUCTED

Experiment Number/Name	***Atmosphere Conditions***	***Heating Sequence***
Exp. 1 - Single Gas and Ramping Rate	Dry Air	Room Temp. - 800℃ (5℃/min)
Exp. 2 - Single Gas and Ramping Rate	Argon	Room Temp. - 800℃ (5℃/min)
Exp. 3 - Mixed Gas	Argon and 5% Dry Air	Room Temp. - 450℃ (5℃/min)
Exp. 4 - Customized Two-Step Heating Sequence	Argon then switched to Dry Air	Step 1 - Room Temp. - 450℃ (5℃/min) Step 2 - 450℃ - 150℃ (5℃/min) Step 3 - Switch Gas to Dry Air Step 4 - 150℃ - 600℃ (5℃/min)
Exp. 5 - Customized Variable Heating Sequence	Dry Air	Step 1 - Room Temp. - 150℃ (5℃/min) Step 2 - 150℃ - 250℃ (1℃/min) Step 3 - 250℃ - 300℃ (5℃/min) Step 4 - 300℃ - 450℃ (1℃/min) Step 5 - 450℃ - 600℃ (5℃/min)
Exp. 6 - Nitrogen	Nitrogen	Room Temp. - 450℃ (5℃/min)

4 - RESULTS

With the TGA and DSC data for weight loss and heat release, thorough analyses were conducted for each experiment to determine the effectiveness of each heating sequence and its corresponding atmospheric conditions. More specifically, the analyses will assist with the identification of regions where reactions are occurring and indicate their impact on weight loss and heat release. When there is excessive heat release or rapid weight loss transpiring, the green body's structure is more likely to suffer defects, as a result of too much binder volatilization happening at once. Ideally, a successful binder burnout process would have no dramatic peaks in heat release and a steady weight loss curve with a small slope, however, those results are difficult to achieve. Based on the analyses, the necessary changes were implemented for each subsequent experiment, with the intention of achieving a successful binder burnout process.

4.1 Benchmark Experiment in Dry Air

Experiment #1 represents the benchmark of this study, in which the LSM sample was heated from room temperature - 800°C at a constant 5°C/min ramping rate within an atmosphere consisting of dry air. The decision to use dry air as the benchmark is based on it being the standard gas of choice for binder burnout processes in industrial environments. Thus, it allows for the benchmark results to accurately reflect binder burnout behavior(s) in a production line. Heating LSM samples under a constant ramping rate in dry air allowed for a careful examination of the sample's response to the gas. The results from this experiment point directly to the nature of the gas within the chamber, which is the major catalyst for the reactions seen in LSM.

In analyzing the weight loss and heat release results gathered from Experiment #1, as shown in Figure 5, three regions were identified, as the regions where reactions appear to occur as indicated by the peaks in the heat release curve. The following three regions suggest that three separate reactions occur during the binder burnout process; an endothermic reaction beginning at approximately 50°C (Peak A) and two exothermic reactions, with the first beginning slightly before 200°C, at approximately 180°C (Peak B) and the other at 350°C (Peak C). The endothermic reaction occurring at 50°C is likely a result of the water evaporating from the LSM sample, as water begins to evaporate between 0°C - 100°C. The following two regions of rapid heat release are likely due to the volatilization and decomposition of the binder species. These regions are

accompanied by two zones of drastic weight loss occurring over the temperature ranges of 150 - 200°C (1.5wt.% loss) and 250 - 350°C (3.5wt.% loss). These regions of rapid weight loss and heat release should be avoided as they would likely result in defects, such as fire cracking, in the specimen.

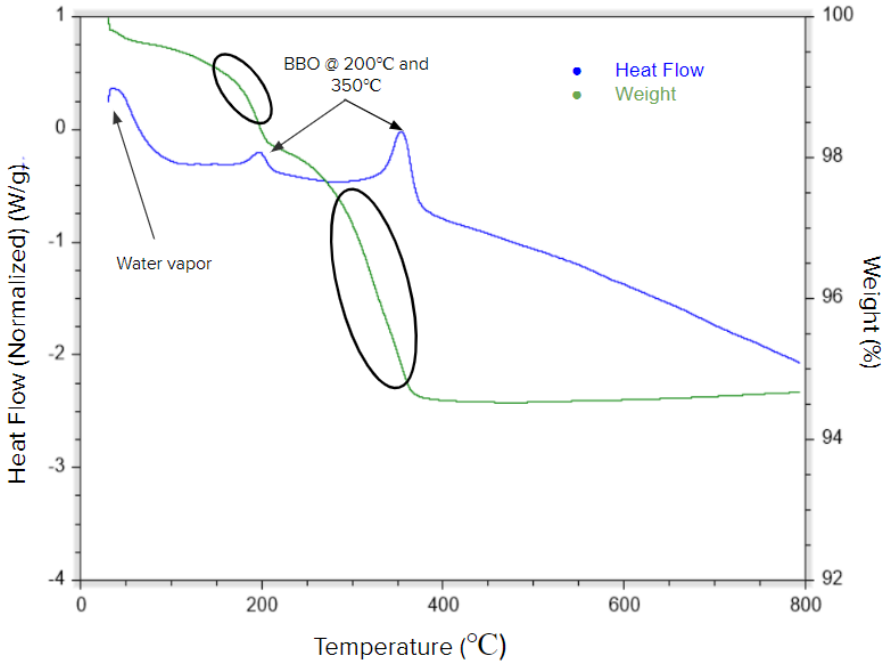

FIGURE 5 – TGA RESULTS OF EXPERIMENT #1 IN DRY AIR

4.2 Exploring Argon as an Alternative Chamber Gas

Since dry air produced undesirable heat release and weight loss rates, new samples were tested under the alternative atmospheric condition of argon. Argon was chosen because it is an inert gas with much lower oxygen partial pressure than dry air. This minimizes the exothermic effect because the absence of oxygen removes the possibility of a combustion reaction taking place between oxygen and the binder. In return, the binder can be burned out without exposing the specimen to the exothermic reactions that cause defects.

When looking at the results from Experiment #2 in argon (see Figure 6), there appears to be a two-step weight loss process occurring in the ranges of 100°C - 210°C (1wt.% loss) and 300°C - 400°C (2.5wt.% loss). There is an observable difference in the intensity of the weight loss in argon versus the weight loss in dry air. The first weight loss region in argon occurs over a 110°C temperature range and the second occurs over a 100°C range. This contrasts dramatically to dry air which

experienced significantly greater weight loss over much shorter temperature ranges. The reduced weight loss and the wider temperature ranges achieved by using argon allows for a more controlled binder removal process. This helps to eliminate dramatic exothermic reactions and is likely to produce fewer defects in the specimen.

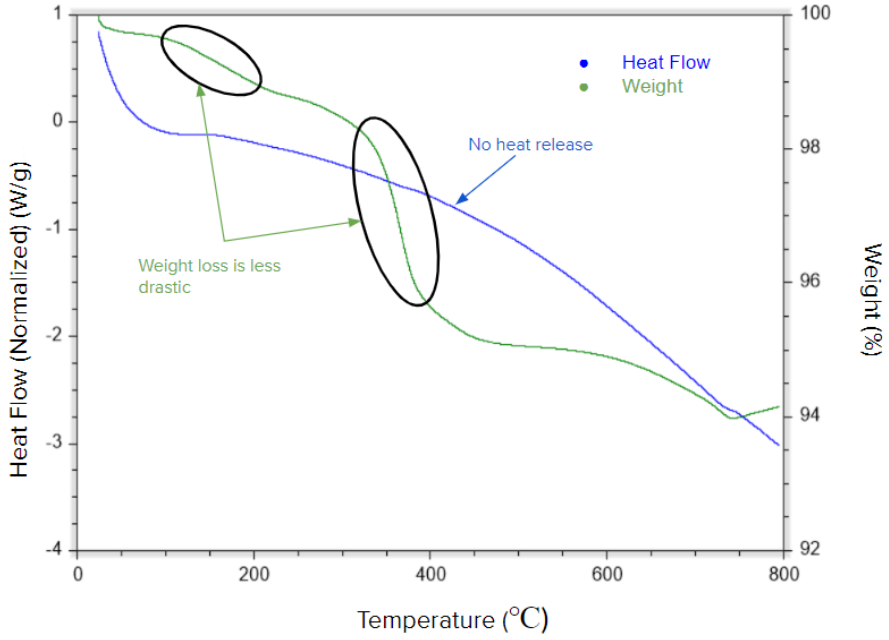

FIGURE 6 – TGA RESULTS OF EXPERIMENT #2 IN ARGON

The heat flow curve in argon, as shown in Figure 6, demonstrates no significant signals of exothermic reactions. The specimen experiences an endothermic reaction first, signaling the evaporation of water, similar to Peak A in Experiment #1. However, this was the only observable reaction that occurred according to the heat curve, dissimilar to Experiment #1 which has Peaks B and C in addition to Peak A. As expected, the limited exposure of the LSM sample to oxygen greatly reduced the reactivity of the binder. This demonstrates the potential of argon to sustain the controlled release of the binder and prevent the occurrence of defects. Without altering the heating sequence, more favorable results were produced by using an inert gas such as argon instead of a more reactive gas, such as dry air with 21% oxygen.

After observing argon's ability to effectively control the heat released, it is essential to test the behavior of LSM under intermediate atmospheric conditions with almost 1% oxygen partial pressure (95% argon and 5% dry air) as done in Experiment #3. The purpose of this experiment is to test the sensitivity of controlling the oxygen partial pressure during binder burnout. It is expected

that this would allow for rapid weight loss, as seen in the benchmark experiment with dry air (Exp. #1), while the argon would allow for the maintenance of a controlled heat release. As seen in Figure 7, these changes to the atmospheric conditions produce a more constant and wider region of weight loss, suggesting that the oxygen concentration in the gas is important. However, there is an intense exothermic reaction at 410°C and a region of rapid weight loss from 300°C - 420°C. When comparing Experiment #3 to Experiments #1 and #2, it becomes apparent that a mixture of dry air and argon reduces the number of exothermic reactions and regions of rapid weight loss present. While using dry air and argon in Experiments #1 and #2 respectively, there were two regions of weight loss, but the specimen under mixed atmospheric conditions only experienced one. However, the single region of weight loss in Experiment #3 is a continuous region of relatively steady weight loss, that only became significant and exhibits some dramatic weight loss after 310°C. It should also be noted that in Experiment #3 there is only one exothermic reaction as opposed to Experiment #1 which has two.

Consequently, the subsequent experiments will involve:

1. Adopting a two-step heating sequence using argon and dry air.
2. Reducing the ramping rate within the exothermic regions where rapid weight loss and dramatic heat release were present in Experiment #1.

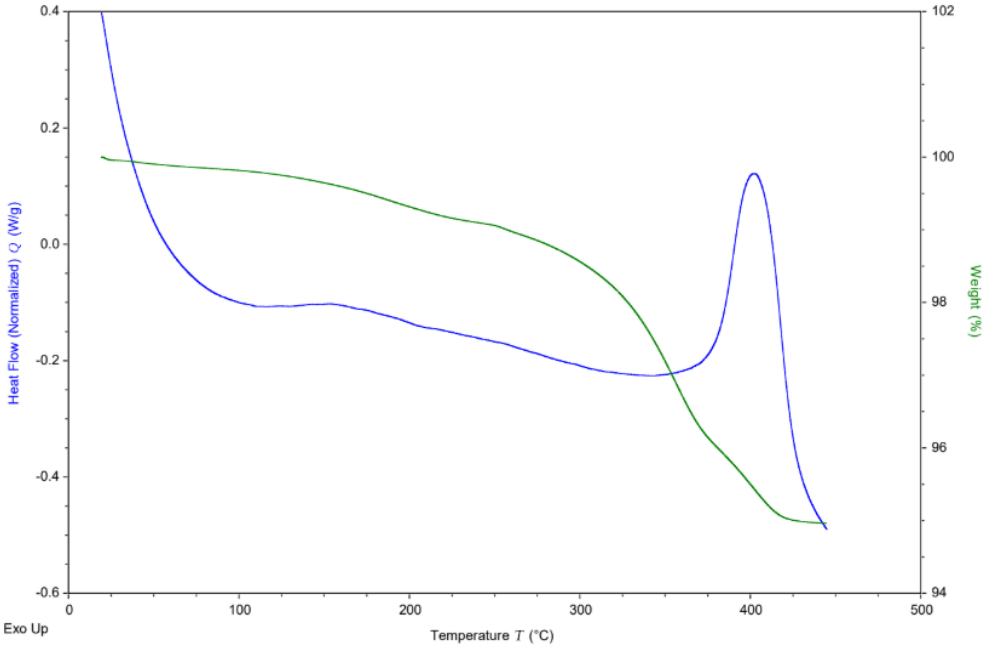

FIGURE 7 – TGA RESULTS OF EXPERIMENT #3 IN THE MIXTURE OF ARGON AND 5% DRY AIR

4.3 Investigation of Two-Step Binder Burnout

After understanding the effects of the mixed gases on LSM, it is of great interest to observe how LSM would react if exposed to argon followed by the more reactive dry air. It is expected to eliminate the dramatic heat peaks caused by the oxygen present in dry air since argon is inert and remove most of the binder material during the first step. For this experiment, LSM was heated in argon with a constant rate of 5°C/min, from room temperature - 450°C, cooled to 150°C and then heated to 600°C in dry air, again with a constant ramping rate of 5°C/min.

Based on the TGA results from Experiment #4, shown in Figure 8, the graph for the argon step displays identical weight and enthalpy changes as Experiment #2. The results for Experiment #4 indicate that there is a two-step weight loss process occurring within the temperature ranges of 100°C - 210°C and 300 - 400°C, with an apparent lack of exothermic reactions. Overall there was a 4.5% decrease in weight under argon, confirming the repeatability of Experiment #2. However, this is followed by observable weight loss during the second step in dry air where an additional 0.5wt.% is removed. This weight is assumed to be residual carbon that remained due to the inert nature of argon and lack of oxygen in the gas chamber. Thus, oxygen reacts with and volatilizes the residual carbon after the chamber gas is switched to dry air.

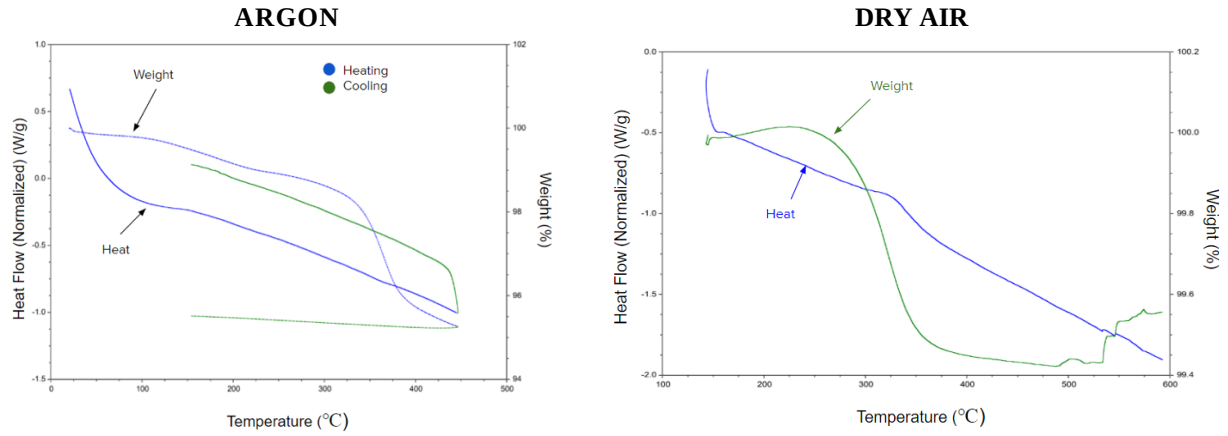

FIGURE 8 – TGA RESULTS OF EXPERIMENT #4 IN ARGON AND DRY AIR

4.4 Customized Variable Heating Sequence

To achieve an ideal binder burnout sequence for LSM, information from Experiment #1 was used to reduce the ramping rate during temperatures associated with rapid weight loss. In this case, the ideal binder burnout sequence would involve gradual weight loss with minimum heat release to reduce damage to the sample. As seen in Figure 5, 200°C and 350°C were identified as critical

temperatures associated with rapid heat release and weight loss in Experiment #1. With this in mind, it is essential to decrease the ramping rates leading up to these temperatures from 5°C/min to 1°C/min to allow for a more detailed investigation of the activity within these temperature ranges. It is important to note that the sudden jumps in heat flow at the points in which the ramping rate is changed do not reflect the actual heat released. TA Instruments SDT 650, the machine used to carry out these TGA experiments, makes corrections in the heat flow scale which causes the appearance of an exothermic jump. According to Figure 10, the resulting enthalpy curve for multiple ramping rates identified 175°C and 325°C as critical temperatures associated with rapid weight loss. The weight loss curves are also less steep and demonstrate a more controlled binder removal process.

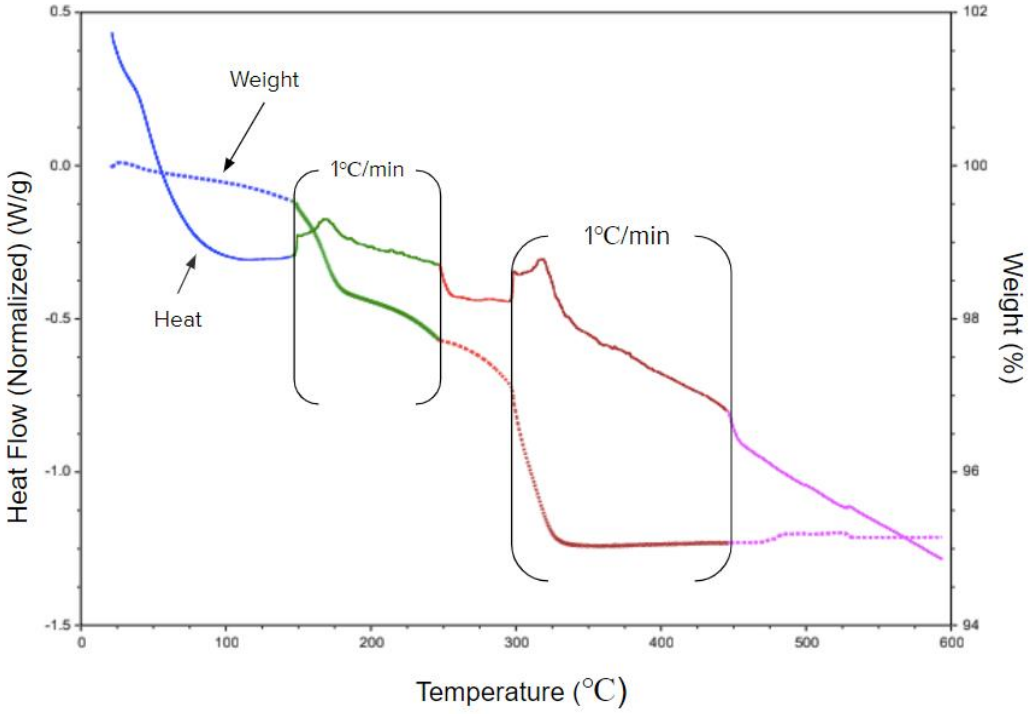

FIGURE 9 – TGA RESULTS OF EXPERIMENT #5 WITH REGIONS OF SLOWED RAMPING RATE OUTLINED

5 - DISCUSSION

Since dry air is commonly used as an atmospheric gas in the industry during binder burnout processes, the results from the dry air, Experiment #1, are used as the baseline for the following analyses. With dry air as the baseline, the relationships between the other experiments' results and dry air can be appropriately scaled and accurately depicted for detailed analysis. Based on the analyses, information was gathered and conclusions were drawn that may result in better optimization of the binder burnout process. However, with the industry standards typically involving lengthy heating sequences that increase costs, the desire to minimize expenses led to an investigation into alternative atmospheric gases. It was recommended to use the inexpensive N_2 gas to save the cost.

5.1 Reducing the Intensity of Weight Loss

When looking specifically at the weight loss results from Experiments #1 through #3 and Experiment #6 and comparing them, as shown in Figure 10, it can be observed that the green body's weight loss behavior depends heavily on the atmospheric conditions used in the burnout process. The ideal weight loss behavior would have a relatively linear slope with a consistent decline because it would allow for most of the binder to be safely removed without creating significant internal pressure. According to Figure 10, dry air is the first to begin the process of rapid weight loss, exhibiting two regions of dramatic weight loss. Upon the completion of burnout, dry air achieves the greatest weight loss, as it is reduced to 94.5% with a total weight loss yield of 5.5%. While dry air removes all of the binder contents, its weight loss curve is far from the ideal, which suggests it will likely suffer defects if it is used without holding temperatures for extended periods of time. Thus, it is essential to obtain a weight loss curve that is closer to the ideal by using alternate atmospheric conditions.

To accurately analyze the binder burnout of LSM in nitrogen, the same heating sequence of room temperature - 450°C at a ramping rate of 5°C/min was used. As seen in Figure 10, the weight loss of the specimen under nitrogen and argon are nearly identical. Considering its lower cost, N_2 gas is recommended.

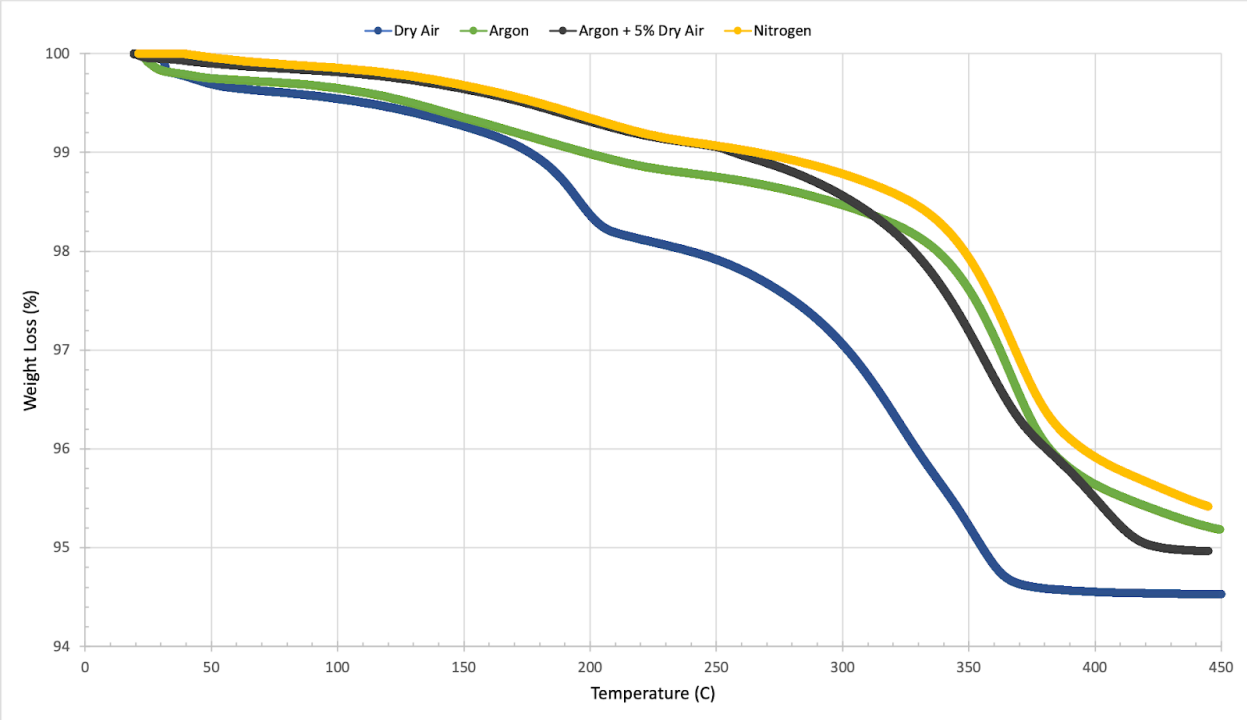

FIGURE 10 – COMPARISON OF WEIGHT LOSS BETWEEN DRY AIR (EXP. #1), ARGON (EXP. #2), THE MIXED GAS (EXP. #3), AND NITROGEN (EXP. #6)

Based on the results, each alternative atmospheric condition achieved more gradual weight loss compared to Experiment #1 where dry air was used, indicating that alternate atmospheric conditions can reduce the intensity of weight loss. It should be noted that Experiment #1 in dry air is the only experiment with two distinct regions of rapid weight loss, while the inert atmospheric conditions generated only one region of weight loss toward the end of the process. However, it is important to note that using alternative atmospheric conditions results in slightly less overall weight loss due to the presence of residual carbon. Therefore, dry air is a reliable choice for complete carbon removal in the binder. Although, the extreme weight loss in dry air makes it unsuitable because these occurrences often lead to defects or even cracks, which is why using dry air after an inert gas will help eliminate this residual carbon and provide a more stable burnout process.

5.2 Reducing the Intensity of Heat Flow

It is important to ensure that the heat flow curve during the burnout process does not experience any observable reactions. In most cases, high peaks of heat release will result in defects because intense reactions can compromise the green body. Through the experiments, dry air was found to

have the most intense heat reactions. This suggests that oxygen plays an important role in heat flow behavior, especially at temperatures greater than 200°C.

Experiment #2 in argon shows a reduced intensity of heat flow compared to Experiment #1, as shown in Figure 11. In Experiment #1 with dry air, there is an endothermic reaction at 50°C and there are two exothermic reactions at 200°C and 350°C. Whereas in Experiment #2, there is one main endothermic reaction at 50°C, the same as dry air, and the remaining heat release is more gradual than in Experiment #1. A reduction in the intensity of the heat flow is important because it means that there will be fewer defects if the heat flow is more gradual.

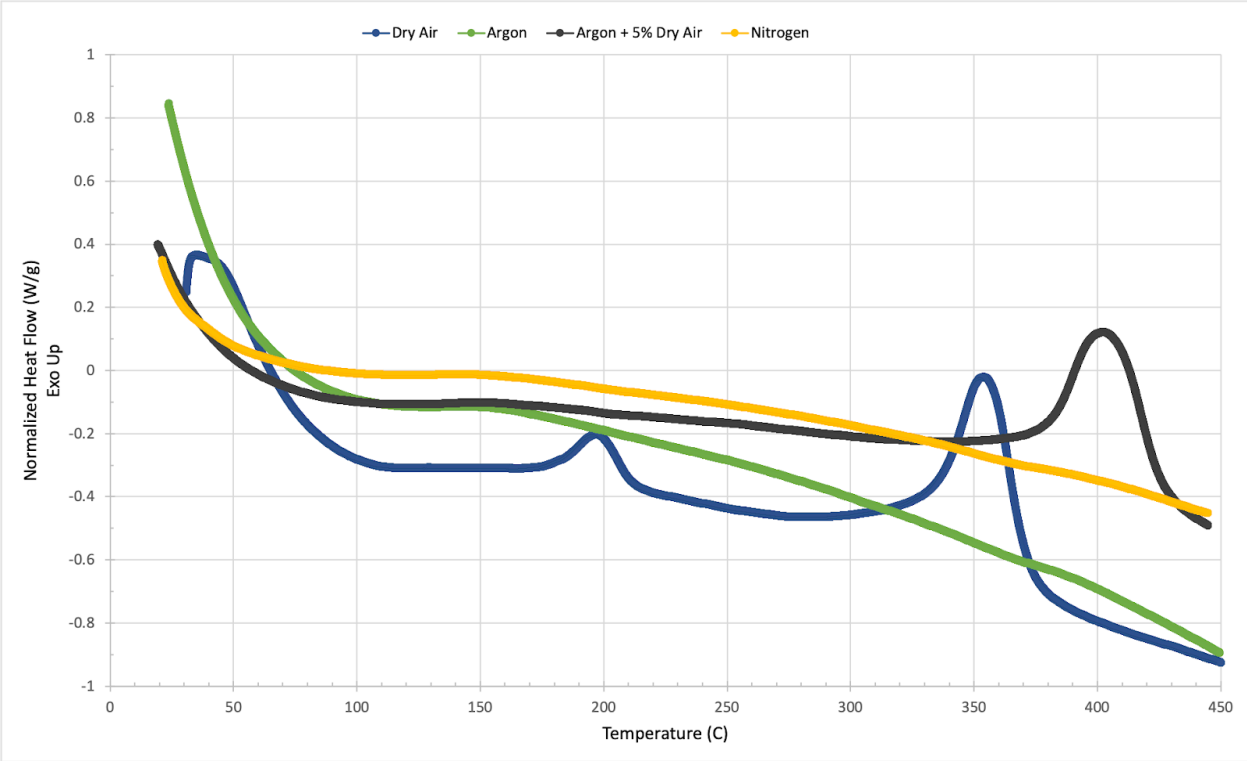

FIGURE 11 – COMPARISON OF NORMALIZED HEAT FLOW BETWEEN DRY AIR (EXP. #1), ARGON (EXP. #2), THE MIXED GAS (EXP. #3), AND NITROGEN (EXP. #6)

Looking specifically at Experiment #3 using mixed gas, there is a reduction in the number of exothermic reactions which ultimately results in a reduction of heat flow compared to Experiment #1 where dry air was used. Comparing Experiments #2 and #3, in addition to Experiment #6, using argon, mixed gas, and nitrogen, respectively, to Experiment #1, using dry air, the curves show that argon, whether it is pure or mixed with dry air and nitrogen are critical for reducing the intensity of heat release in the different experiments. Henceforth, both argon and nitrogen make for the

desirable atmospheric conditions because they accomplish the objectives of reducing the intensity of the weight loss and the heat flow.

5.3 Multiple Ramping Rates

It is common for companies producing SOFCs to use multiple ramping rates throughout the binder burnout process. This has proven to be a reliable method of controlling internal pressures and heat flow in order to prevent defects. However, through the results, it is apparent that there is room for improvement in the industry-standard heating sequence. The results have shown that lowering the ramping rate in areas of rapid heat release and weight loss successfully reduces the intensity of heat release and weight loss.

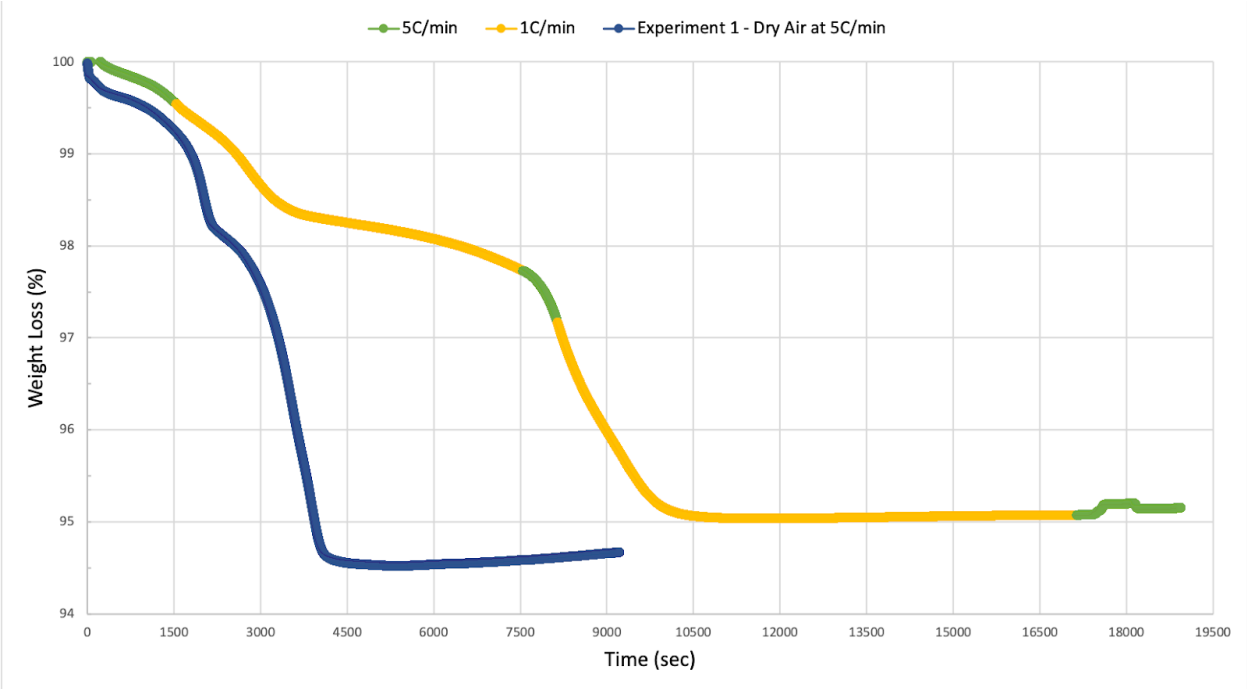

FIGURE 12 – COMPARISON OF WEIGHT LOSS BETWEEN EXP. #1 AND EXP. #5 (WITH RESPECT TO TIME)

According to Figure 12, the slopes within the 1°C/min range were less steep than those shown in the results for 5°C/min in dry air. Likewise, by reducing the ramping rate in exothermic regions, the observable heat flow peaks were significantly reduced as seen in Figure 13. These smaller exothermic reactions are less likely to produce defects than those shown in Experiment #1. It can be seen that using a 1°C/min ramping rate gives a more detailed view of the heat flow and weight loss behavior experienced during exothermic reactions. The results shown in Section 4.4, Figure

9 show that the 1°C/min regions could be shortened by approximately 50°C and still contain the reaction within it. Making these changes to the heating sequence ensures the stability of the green body and reduces production time. Even though the heating sequence itself is more time consuming, it provides the advantage of a more steady burnout process.

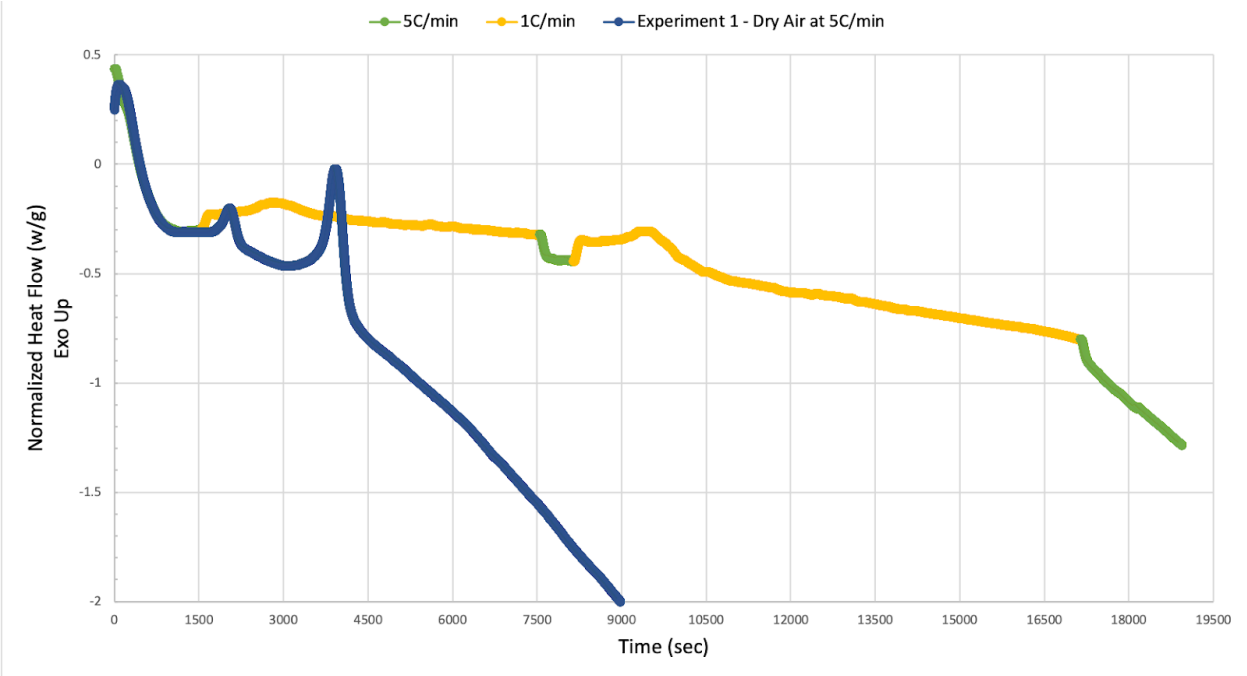

FIGURE 13 – COMPARISON OF NORMALIZED HEAT FLOW BETWEEN EXP. #1 AND EXP. #5 (WITH RESPECT TO TIME)

5.4 Two-Step Heating Sequence

Another option to help reduce the intense weight loss is to separate it into two steps, using argon first to remove most of the binder with a gradual weight loss and then switching to dry air to remove the residual carbon. Figure 14 shows the comparison of weight loss between Experiment #1 using only dry air and Experiment #4 using argon and then dry air in a two-step binder burnout process. From the results it is evident that the weight loss in the first step, with argon, is more gradual than dry air and can help avoid those defects caused by intense weight loss. In the second step with dry air, there is a small amount of weight loss that occurs gradually, due to the residual carbon being removed. Therefore, the total weight loss from Experiment #4 is very similar to the total weight loss of Experiment #1, and the two-step process has the added benefit of defects being less likely to occur.

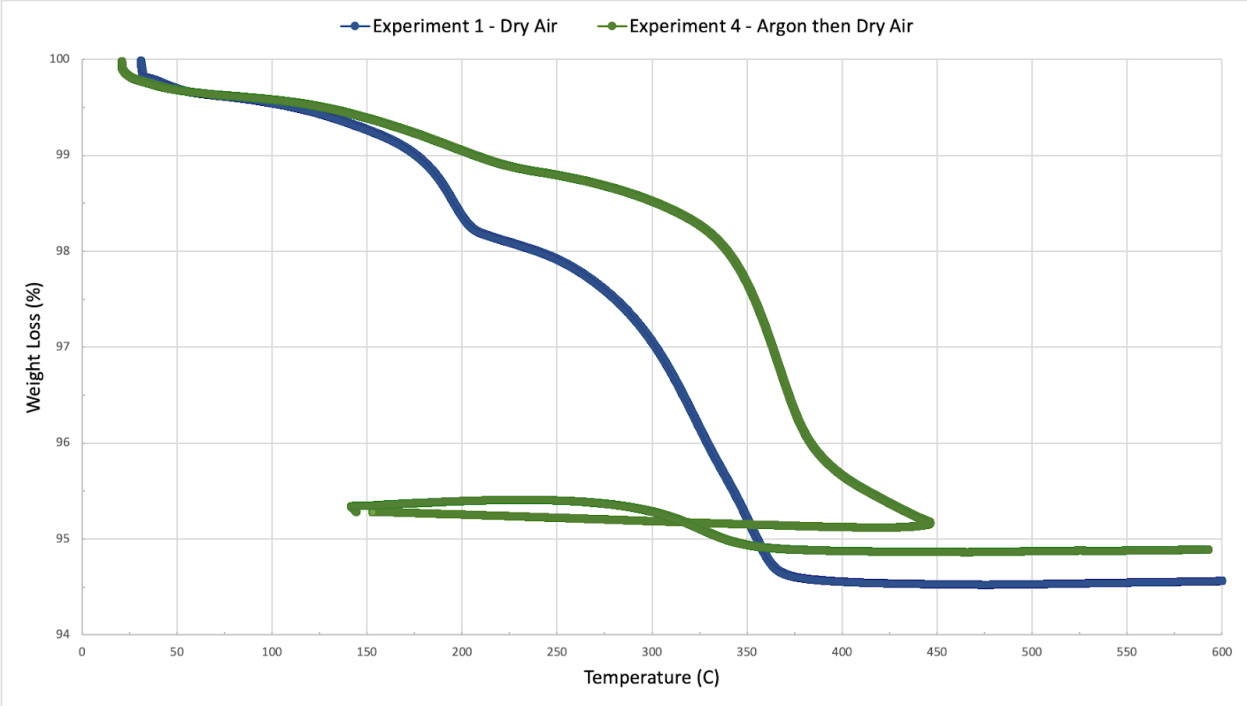

FIGURE 14 – COMPARISON OF WEIGHT LOSS BETWEEN DRY AIR (EXP. #1) & ARGON AND THEN DRY AIR (EXP. #4)

6 - Conclusions & Recommendations

The goal of this project was to reduce the time necessary for the binder burnout process while ensuring defects do not occur. After conducting extensive research, a series of experiments, and detailed analyses of the results, the team arrived at multiple conclusions and developed a diverse range of recommendations for industry application.

While dry air is the industry standard atmospheric condition used for binder burnout, the results of the benchmark experiment (Experiment #1) indicate that using dry air induces dramatic and swift weight loss as well as spikes in the heat release, which is extremely undesirable and likely what induces the propagation of defects. In an attempt to prevent rapid weight loss and minimize the heat release, the team designed various experiments utilizing alternative atmospheric conditions and customized heating sequences. Based on the results where a reducing gas or combination gas was used, such as argon (Experiment #2), argon and 5% dry air (Experiment #3), and nitrogen (Experiment #6), the weight loss and heat release are both reduced significantly and occur more gradually when compared with dry air. Although it is important to note that when using the mixed gas of argon and 5% dry air, there is still a spike in the heat release that is slightly less dramatic than the one seen in dry air within the same temperature range (approximately 350°C - 400°C). Therefore, the team concluded that the binder burnout process is sensitive to oxygen in the atmosphere and recommends the use of a reducing gas, (preferably nitrogen for its affordability) for the binder burnout process to prevent having substantial heat release and weight loss.

Aside from using a reducing gas in place of dry air, the results from Experiment #5 indicate that the implementation of a customized heating sequence that employs variable ramping rates allows for a more stable binder burnout process in dry air than one that employs a constant ramping rate. This method, however, does not necessarily reduce the time for completion of the binder burnout process, as the comparison of the amount of time it takes for the process to occur at a constant ramping rate (Experiment #1) versus the time with variable ramping rates (Experiment #5) indicates that the customized heating sequence required approximately twice the amount of the time. Nevertheless, the team concluded that the benefits of using a customized heating sequence, in which the ramping rates are tailored as needed to address and stabilize the regions of concern, outweighs the extension of time. Thus, if dry air is still being used as the atmospheric condition,

the team recommends utilizing a customized heating sequence with variable ramping rates.

At last, the team came to the conclusion that addressing a binder burnout heating sequence with a two-step approach resulted in the desired gradual weight loss and heat release. When using the two-step approach as outlined in Experiment #4, there is still some residual carbon present following the completion of the argon step, indicating that there is potential for more weight loss to occur. When comparing the weight loss from the two-step approach, (Experiment #4), to the weight loss of pure dry air, (Experiment #1), the total weight loss is exceptionally similar. Henceforth, by using dry air in the second step, since binder burnout is sensitive to oxygen, it allows for the removal of that residual carbon. Therefore, the team recommends using a two-step approach for binder burnout, because it too can deliver comparable weight loss and presents the same benefits of having gradual heat release and weight loss.

To confirm the validity of these different approaches for optimized binder burnout, the team recommends that further experiments are conducted on large scale samples to understand how size can impact the process since the samples used in these experiments were very small. Developing a more precise region-specific customized heating sequence would be helpful in identifying and isolating the temperatures where areas of dramatic heat release and weight loss occur. Lastly, the team recommends future work focused on creating a computer-generated model, based on the results, as a mechanism to predict future experiments and potential heating sequences.

REFERENCES

Alford, N. M., Birchall, J. D., & Kendall, K. (1986). Engineering ceramics - the process problem. *Materials Science and Technology, 2*(4), 329-336. 10.1179/mst.1986.2.4.329

Beyler, C. L., & Hirschler, M. M. (2002). Thermal decomposition of polymers. *SFPE Handbook of Fire Protection Engineering, 2*

Dash, C. (2011). *Synthesis of Lithium Titanate By Auto Combustion Method and Study of its Densification Behavior with Different Binder Concentration*

Donzel, L., Mannes, D., Hagemeister, M., Lehmann, E., Hovind, J., Kardjilov, N., & Grünzweig, C. (2018). Space-resolved study of binder burnout process in dry pressed ZnO ceramics by neutron imaging. *Journal of the European Ceramic Society, 38*(16), 5448-5453. 10.1016/j.jeurceramsoc.2018.08.017

Enneti, R. K., Park, S. J., German, R. M., & Atre, S. V. (2012). Review: Thermal Debinding Process in Particulate Materials Processing. *Materials and Manufacturing Processes, 27*(2), 103-118. 10.1080/10426914.2011.560233

Ewsuk, K. G., Cochran, R. J., Blackwell, B. F., Cesarano, J., & Adkins, D. R. (1995). *Experimentally Validated Computational Modeling of Organic Binder Burnout from Green Ceramic Compacts.* Albuquerque, NM: Sandia National Laboratories.

Gonzalez-Gutierrez, J., Stringari, G., & Emri, I. (2012). Powder Injection Molding of Metal and Ceramic Parts. (pp. 79-80)10.5772/38070

Incledon, M. L. (2013). *Modeling binder removal in ceramic compacts* Available from Masters Abstracts International http://www.pqdtcn.com/thesisDetails/DBD6F1CF2DE7415D23314873D236F455

Lewis, J. A. (2001). Organic Processing Additives. In K. H. J. Buschow, R. W. Cahn, M. C. Flemings, B. Ilschner, E. J. Kramer, S. Mahajan & P. Veyssière (Eds.), *Encyclopedia of Materials: Science and Technology* (pp. 6556-6560). Elsevier. https://doi.org/10.1016/B0-08-043152-6/01159-1

Maleksaeedi, S., & Moritz, T. (2018). Additive manufacturing of ceramic materials. In J. Zhang, & Y. Jung (Eds.), *Additive Manufacturing: Materials, Processes, Quantifications and Applications* (pp. 105-156). Butterworth-Heinemann, 2018. 10.1016/B978-0-12-812155-9.00004-9

Mason, T. (2016). Advanced Ceramics. *Encyclopedia Britannica,* https://www.britannica.com/technology/advanced-ceramics

Mezquita, A., Monfort, E., Vaquer, E., Ferrer, S., Aranal, M. A., Toledo, J., & Cuesta, M. A. (2012). Energy optimization in ceramic tile manufacture by using thermal oil. *Boletin de la Sociedad Espanola de Ceramica y Vidrio, 51*(4), 183-190. http://inis.iaea.org/search/search.aspx?orig_q=RN:43111482

Moeggenborg, K. J., & Reed, P. E. (2002). In Ecolab USA Inc. (Ed.), *Polymeric binders for ceramic processing*

Niesz, D. E. (1996). A Review of Ceramic Powder Compaction. *KONA Powder and Particle Journal, 14*, 44-51. 10.14356/kona.1996009

Pollinger, J. P., & Messing, G. L. (1985). Thermal Analysis of Organic Binders for Ceramic Processing. In R. L. Snyder, R. A. Condrate & P. F. Johnson (Eds.), *Advances in Materials Characterization II* (pp. 359-370). Springer US. 10.1007/978-1-4615-9439-0_28

Reed, J. (1995). *Principles of Ceramics Processing* (2nd ed.). John Wiley & Sons, INC (US).

Salehi, M., Clemens, F., Graule, T., & Grobéty, B. (2012). Kinetic analysis of the polymer burnout in ceramic thermoplastic processing of the YSZ thin electrolyte structures using model free method. *Applied Energy, 95*, 147-155. https://core.ac.uk/download/pdf/20662117.pdf

Santos, M. A. d., Neivock, M. P., Maliska, A. M., Klein, A. N., & Muzart, J. L. R. (2004). Plasma debinding and pre-sintering of injected parts. *Materials Research, 7*(3), 505-511. 10.1590/S1516-14392004000300021

Shanefield, D. J. (1995). Binders. In D. J. Shanefield (Ed.), *Organic Additives and Ceramic Processing: With Applications in Powder Metallurgy, Ink, and Paint* (pp. 255-279). Springer US. 10.1007/978-1-4757-6103-0_9

Wolff, H. (2018). Ronald (Ron) Charles Garvie [1930-1991]. https://csiropedia.csiro.au/ronald-garvie/

Zhang, T., Blackburn, S., & Bridgwater, J. (1996). Debinding and sintering defects from particle orientation in ceramic injection moulding. *Journal of Materials Science, 31*(22), 5891-5896. 10.1007/BF01152138